Work Generation from Thermal Noise by Quantum Phase-Sensitive Observation

Tomas Opatrný,[1] Avijit Misra,[2,3,*] and Gershon Kurizki[3]

[1]*Department of Optics, Faculty of Science, Palacký University, 17. listopadu 50, 77146 Olomouc, Czech Republic*
[2]*International Center of Quantum Artificial Intelligence for Science and Technology (QuArtist) and Department of Physics, Shanghai University, 200444 Shanghai, China*
[3]*Department of Chemical and Biological Physics, Weizmann Institute of Science, Rehovot 7610001, Israel*

(Received 11 November 2020; revised 21 March 2021; accepted 16 June 2021; published 20 July 2021)

We put forward the concept of work extraction from thermal noise by phase-sensitive (homodyne) measurements of the noisy input followed by (outcome-dependent) unitary manipulations of the postmeasured state. For optimized measurements, noise input with more than one quantum on average is shown to yield heat-to-work conversion with efficiency and power that grow with the mean number of input quanta, the efficiency and the inverse temperature of the detector. This protocol is shown to be advantageous compared to common models of information and heat engines.

DOI: 10.1103/PhysRevLett.127.040602

Introduction.—The highest entropy at a given energy pertains to thermal noise, which is a ubiquitous form of energy in the Universe [1]. Since work [2,3] is an "ordered" form of energy, delivered *without entropy change* [4–8], a thermal ensemble of oscillators stores heat but not work. Here, we propose an efficient way to harness such ensembles for fast performance of useful work. Classically, the protocol appears to be straightforward: impulsively observe the phase and amplitude of each oscillator (via two "snapshots" at a chosen time interval), wait until it is in full swing, then let it discharge its stored work [Fig. 1(a)]. Yet, what is the quantum mechanical (QM) counterpart of this protocol? Any noisy ensemble of QM harmonic oscillators at a given frequency (mode) forms a random distribution of coherent states. Therefore, our QM protocol invokes homodyne measurements [1,9–16] optimized to approximately reveal a coherent-state component of the random distribution and thereby sample the quadratures of the oscillator field within the uncertainty-limit accuracy. We show that unitary manipulations of the postmeasured state that are determined by the measurement outcome can yield heat-to-work conversion at an efficiency that grows with input temperature.

This protocol introduces the concept of exploiting *randomly distributed, noncommuting, continuous variables* as thermodynamic resources for work extraction by estimating their quadrature values *at minimal energy cost*. We dub the concept "work by observation and feedforward" (WOF).

WOF engine principles.—We consider an input state of a harmonic oscillator, e.g., a single electromagnetic field mode, whose phase-space distribution falls off monotonically and isotropically from its zero-energy (vacuum) origin [9,11], as in the case of the Gaussian thermal state. Such a QM state, dubbed "passive" [4], is incapable of delivering work by unitary transformations. It must be rendered nonpassive to allow for subsequent work extraction from its stored work (alias ergotropy) by a unitary process [5–7,17–22] [see Supplemental Material (SM), I [23]]. A standard homodyne measurement can transform this passive state into a nonpassive coherent state by mixing it with a much stronger, coherent, local oscillator (LO) [9–14]. Yet, to extract maximal work, the measurement should consume as little energy as possible. How can this be achieved?

To this end, we propose a nonstandard homodyne measurement that only probes a split-off small fraction of the thermal input field by mixing it with an LO as weak as this fraction [Fig. 1(b)]. This measurement yields quadrature values of the field with optimal trade-off between energy cost and precision. The measurement outcome serves to determine the unitary operations that extract maximal work from the postmeasured output: a "downshift" (displacement) toward the zero-energy origin, supplemented by "unsqueezing" [Fig. 1(c)]. The downshift can be realized by adjusting the transmissivity and phase delay of a beam splitter (or an amplitude-phase modulator) according to the outcome. The output-field quadratures are then shifted by this beam splitter to make the output constructively interfere with the coherent field in the working mode [Figs. 2(a) and 2(b)]. For $\bar{n} \gg 1$, $\bar{n}$ being the mean number of input quanta, nearly the *entire energy* of the thermal ensemble is shown to be extractable as work, with efficiency $1 - O(1/\sqrt{\bar{n}})$, by a *single* optimized homodyne measurement. The energy cost that may limit the WOF efficiency is accounted for, the fundamental cost being the detector-record erasure (resetting) cost [26–31].

The WOF scheme is feasible and conceptually simple [Fig. 1(c), Figs. 2(a) and 2(b)]. It is shown to be advantageous compared to Szilard or Maxwell-demon information engines based on binary measurements of discrete variables

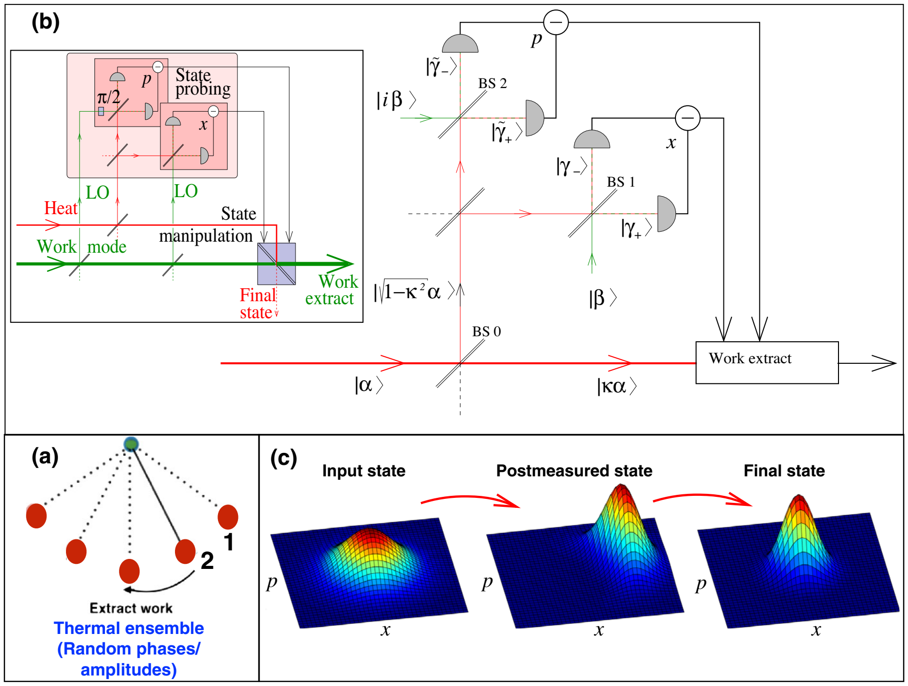

FIG. 1. (a) Work extraction by snapshots (1, 2) from a random ensemble of pendula. (b) WOF scheme for a thermal mixture of coherent states $|\alpha\rangle$). A homodyne measurement (see text) is performed on the reflected, weak part of the input superposed with a (comparably weak) local oscillator (LO) to optimally estimate the quadratures x and p. The result is used to adjust the output to constructively interfere with the LO and thereby downshift it to extract work. (c) A thermal mixture of coherent states is transformed by the measurement to a displaced, squeezed (slightly non-Gaussian) state. Work is extracted by displacement and unsqueezing to a state with much less energy than the postmeasured state.

[32–44]. It can also outperform common models of heat engines that exploit the same resources (see "Discussion").

Work extraction and its bounds.—Any single-mode input state can be represented as $\hat{\varrho} = \int\int P(\alpha)|\alpha\rangle\langle\alpha|d^2\alpha$, P, being the Glauber-Sudarshan distribution function of coherent states $|\alpha\rangle$ with complex amplitudes α [11–14]. Let us first consider a coherent-state component $|\alpha\rangle$ of the input distribution [Fig. 1(b)]. After the 0th beam splitter (BS0) with high transmissivity κ, the state $|\kappa\alpha\rangle$ is transmitted and the state $|\sqrt{1-\kappa^2}\alpha\rangle$ (that has a much smaller amplitude) is reflected (split off) toward the homodyne detectors. These detectors serve for estimating the quadrature operators $\hat{x}$ and $\hat{p}$, $\hat{x} = 2^{-1/2}(\hat{a} + \hat{a}^\dagger)$, and $\hat{p} = -2^{-1/2}i(\hat{a} - \hat{a}^\dagger)$, where $[\hat{a}, \hat{a}^\dagger] = 1$ (here we set $\hbar = \omega = 1$). To effect the estimations, the small split-off fractions are superposed at the detectors with two LOs at the same frequency ω. The two LOs (originating from a common source) are prepared by two beam splitters (BS1 and BS2) and a $\pi/2$ phase shifter in coherent states $|\beta\rangle$ and $|i\beta\rangle$ with orthogonal quadrature amplitudes, β chosen to be real numbers [Fig. 1(b)]. Behind BS1 and BS2, we then have a 4-mode coherent state $|\psi\rangle = |\gamma_+\rangle|\gamma_-\rangle|\tilde{\gamma}_+\rangle|\tilde{\gamma}_-\rangle$ with amplitudes $\gamma_\pm = (1/\sqrt{2})\times[\sqrt{(1-\kappa^2/2)}\alpha \pm \beta]$ and $\tilde{\gamma}_\pm = (1/\sqrt{2})[\sqrt{(1-\kappa^2/2)}\alpha \pm i\beta]$. The photodetection of states $|\gamma_\pm\rangle$ and $|\tilde{\gamma}_\pm\rangle$ yields Poissonian statistics with mean values $\bar{n}_\pm = |\gamma_\pm|^2$ and $\bar{\tilde{n}}_\pm = |\tilde{\gamma}_\pm|^2$, respectively. A homodyne measurement [9,11–16] consists of recording photocount differences between the two pairs of detectors: $\Delta n_x \equiv n_+ - n_-$ and $\Delta n_p \equiv \tilde{n}_+ - \tilde{n}_-$. These Δn_x and Δn_p carry information on the quadrature eigenvalues x and p, since $\bar{n}_\pm$ and $\bar{\tilde{n}}_\pm$ and their variances depend on $\alpha = (1/\sqrt{2})(x + ip)$ (SM, II [23]).

The probability distribution for Δn_x and Δn_p, on condition that the input state was $|\alpha\rangle$, $P(\Delta n_x, \Delta n_p|\alpha) = P(\Delta n_x|\alpha)P(\Delta n_p|\alpha)$, can be inverted by means of the Bayes rule. The postmeasurement state conditional on Δn_x and Δn_p that characterizes the unmeasured (transmitted) part of the output for *any distribution* $P(\alpha)$ then has the form

$$\hat{\varrho}(\Delta n_x, \Delta n_p) = \frac{1}{\kappa^2}\int\int P\left(\frac{\alpha}{\kappa}\middle|\Delta n_x, \Delta n_p\right)|\alpha\rangle\langle\alpha|d^2\alpha. \quad (1)$$

We start from a thermal state with Gaussian $P(\alpha)$, but the resulting state is in general a nonpassive state (unless $\Delta n_x = \Delta n_p = 0$) [Fig. 1(c)].

The measured Δn_x and Δn_p determine the required downshift (displacement) of the output state toward a state whose mean quadratures are zero. This yields work extraction in the amount $W(\Delta n_x, \Delta n_p)$ (SM, II [23]). The mean work obtained following such displacement

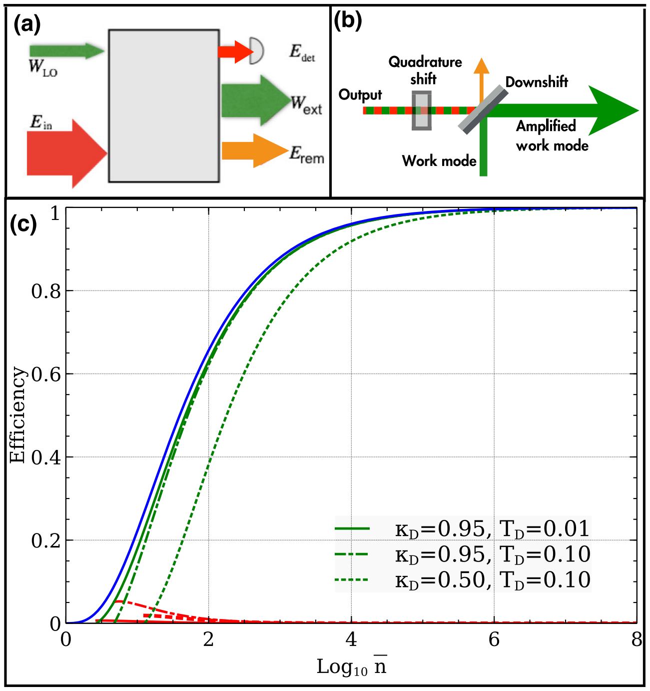

FIG. 2. (a) Energy balance of the WOF scheme. The passive input state has mean energy $E_{\mathrm{in}} = \hbar\omega\bar{n}$; the local oscillators (LO) have mean energy $E_{\mathrm{LO}} = 2\hbar\omega\beta^2$. The detectors absorb energy E_{det}. W is extracted by the displacement and unsqueezing of the unmeasured main fraction of the input. The remaining energy E_{rem} (orange) is unexploitable as work. Work change: green; heat exchange: red. (b) Work extraction by beam-splitter transmittance and phase-shift changes causing constructive interference of the output with the coherent working mode. Orange arrow: remaining (typically thermal) passive output. (c) WOF efficiency as function of $\mathrm{Log}_{10}\bar{n}$ [Eq. (5)]: the bound $\eta^{(1)}_{\max}$ (blue) and actual η for different κ_D and scaled detector temperatures $T_D \leftrightarrow k_B T_D/\hbar\omega$ (green solid, dashed dot, dotted, and dashed). The red lines show $Q_{\mathrm{reset}}/E_{\mathrm{in}}$ for the same parameter values as their green counterparts. Depending on κ_D, the impact of the resetting cost Q_{reset} on the efficiency is seen to be negligible for sufficiently large $\bar{n}$. In these plots, the thermal noise in the local oscillator (LO) and the detectors has mean photon numbers $\bar{n}_{\mathrm{LO}} = \bar{n}_{\mathrm{D}} = 0.05$ (see SM, V [23]).

but ignoring the resetting cost of the detectors (considered below) can be found by averaging $W(\Delta n_x, \Delta n_p)$ over the probability distribution $P(\Delta n_x, \Delta n_p)$ and subtracting the invested mean energy of the two orthogonal-quadrature LOs $2\hbar\omega\beta^2$ to yield the mean work

$$W = \sum_{\Delta n_x}\sum_{\Delta n_x} W(\Delta n_x, \Delta n_p) P(\Delta n_x, \Delta n_p) - 2\hbar\omega\beta^2. \qquad (2)$$

Under the Gaussian approximation (SM, II [23]), one can analytically maximize this extractable mean work with respect to the BS0 transmissivity κ and the intensity β^2 of the LO. This maximization of the mean work in Eq. (2) yields (SM, III [23])

$$W_{\max} \approx \hbar\omega\left(\sqrt{\bar{n} - \sqrt{\bar{n}} + 1} - 1\right)^2 \left(1 - \frac{1}{\sqrt{\bar{n}}}\right). \qquad (3)$$

Equation (3) indicates that mean work extraction ($W_{\max} > 0$) by WOF requires thermal input with $\bar{n} > 1$. For $\bar{n} \gg 1$, the optimal LO $\beta^2 \sim \sqrt{\bar{n}}$ is *much weaker* than the *input* signal, the opposite of standard homodyning [9,11].

A displacement transformation that maximally downshifts the postmeasured state in energy does not fully extract the work from it, since the downshifted state is generally not passive and still keeps work capacity (ergotropy; see SM, I [23]). To extract more work, we can apply an "unsqueezing transformation" (by a Kerr medium [12–14]) to the downshifted state that is centered at the origin, with $\langle x\rangle = \langle p\rangle = 0$. This state has a mean energy of $E_0 = (\hbar\omega/2)(\langle\hat{x}^2\rangle + \langle\hat{p}^2\rangle) = (\hbar\omega/2)(V_+ + V_-)$, where $V_\pm$ are the eigenvalues of the variance matrix of $\hat{x}$ and $\hat{p}$ (SM, IV [23]). The minimal energy state attainable by unsqueezing has the energy $E_{\min} = \hbar\omega\sqrt{V_+ V_-}$ with $V_+ = V_-$. Upon averaging the work extractable by unsqueezing, $W_{\mathrm{US}}(\Delta n_x, \Delta n_p) = E_0 - E_{\min}$, over all measured values of Δn_x and Δn_x, we find that the work in Eq. (2) increases on account of W_{US} by 18% for $\bar{n} = 2$, 12% for $\bar{n} = 5$, and so on: W_{US} *only matters for small* $\bar{n}$ (SM, IV [23]).

Hence, *at high temperature* ($\bar{n} \gg 1$), the maximal work extraction from an input with mean energy $E_{\mathrm{in}} = \hbar\omega\bar{n}$ coincides with the work by displacement in Eq. (3), which reduces to

$$W_{\max} \approx \hbar\omega\left[\bar{n} - 4\sqrt{\bar{n}} + 6 + O\left(\frac{1}{\sqrt{\bar{n}}}, \frac{1}{\bar{n}}\right)\right]. \qquad (4)$$

The $4\hbar\omega\sqrt{\bar{n}}$ cost is the sum of the LO energy $E_{\mathrm{LO}} \approx \hbar\omega\sqrt{\bar{n}}$, the input energy fractions absorbed by the detectors $E_{\mathrm{abs}} \approx \hbar\omega\sqrt{\bar{n}}$, and the remaining (unexploited) output energy $E_{\mathrm{rem}} \approx 2\hbar\omega\sqrt{\bar{n}}$. This E_{rem} corresponds to the (typically thermal) output fluctuations and reflects the fact that our approximate measurement prepares a mixed state that cannot be unitarily transformed to the vacuum state.

The process outlined above can be iterated to exploit E_{rem} for more work extraction and higher efficiency, taking at the kth step $E^{(k)}_{\mathrm{rem}} = \hbar\omega\bar{n}_k = 2\hbar\omega\sqrt{\bar{n}_{k-1}}$ for $k = 1, \ldots, N$. We should stop the N iterations for $\bar{n}_k$ just barely above 1, at which point only negligible work is added, $W^{(k)}_{(\max)} \approx \hbar\omega(\bar{n}_k - 1)^3/32$. Practically, these iterations do not significantly increase the work output (SM, III [23]).

To sustain WOF operation, we must reset the detectors after each work-extraction step. The energy cost of such resetting [26–31], Q_{reset}, sets the fundamental threshold of

WOF to be $W_{\rm net} = W - Q_{\rm reset} > 0$. Detector resetting to the initial temperature T_D requires a minimal energy $Q_{\rm reset} = I k_B T_D \ln 2$, where I is the mean information stored (in bits) by the detectors (SM, VI [23]). For $\bar{n} \gg 1$, $I \simeq \frac{1}{2}\ln(\bar{n}/4)$. Since only a small fraction of the signal is detected ($\Delta\bar{n}_d$ quanta in SM, VI [23]), $Q_{\rm reset}$ is negligible compared to the mean input energy $E_{\rm in} = k_B T$ when $\bar{n} \gg 1$ and $T \gg T_D$. The resetting cost scales much slower (in orders of magnitude) with $\bar{n}$ than the work [Fig. 2(c) and Fig. S8 in SM, VI [23]].

The WOF efficiency, defined as the ratio of the net work output to the heat input, is bounded after the first measurement by

$$\eta = \frac{W_{\rm net}}{E_{\rm in}} < \eta_{\rm max}^{(1)} = \frac{W_{\rm max}}{E_{\rm in}}. \quad (5)$$

Equation (5) refers to the fundamental ("internal") WOF efficiency η. The heat-to-work conversion threshold is $\eta > 0$. Imperfect photodetector efficiency ($\kappa_D^2 < 1$) and finite temperature ($T_D > 0$) obviously raise this threshold (SM, V [23]). As seen from Fig. 2(c) (Fig. S8 in SM, VI [23]), the WOF threshold and efficiency are close to the maximal bound in Eq. (5) for existing highly efficient and cold photodetectors [45,46].

Discussion.—We have introduced a simple scheme for WOF: the hitherto unexplored heat-to-work conversion via information acquisition on *continuous variables* of random (quantum or classical) single-mode fields. The WOF scheme adheres to the laws of thermodynamics: part of the thermal input energy is transferred to the working mode with much less entropy than the input mode; the rest of the entropy is distributed between the detectors and the unexploited (remaining) output. WOF can be thought of as an information-based maser or laser: an amplifier of coherent signals at the expense of information that allows the extraction of the quadrature values of a thermal pump (input). Its efficiency is defined analogously to that of a laser or maser [12] as the ratio of the output (signal) to the input (pump) energy.

At the heart of WOF is the ability to estimate the quadratures at minimal energy cost. Unlike standard homodyning [9,11,15,16], the local oscillator (LO) and the measured field are chosen to be *small fractions* $\sim\sqrt{\bar{n}}$ of the mean input $\bar{n}$, optimizing the work-information trade-off. In order to extract maximal power and work [within the bounds of Eq. (5)], the WOF protocol duration must only exceed the resetting time $\tau_{\rm reset}$ of the detectors to their initial temperature T_D (SM, VI [23]) [47]. In existing photodetectors [45,46], $\tau_{\rm reset} \gtrsim 10$ nsec at the cost of $\sim$10 times the detected photon energy $\hbar\omega$. To boost the power, $\tau_{\rm reset}$ can be made much shorter than the natural relaxation time of the excited detector level (or band) by resetting in the non-Markovian anti-Zeno regime [48–51] at a modest energy cost $\sim\hbar/t_C \ll \hbar\omega$, where t_C is the correlation (memory) time of the environment.

Although their principle of operation is completely different, it is instructive to compare the performance of WOF and heat engines (HEs) to similar resources. For this, let us assume that both engines are energized by a hot bath with the energy $E_{\rm in} = k_B T_h$ and the HE cold bath is chosen to have the energy $k_B T_c = E_{\rm rem}$ [Eq. (5)] (although $E_{\rm rem}$ may not be associated with a genuine cold bath). By this choice, the idealized HE Carnot bound at the reversibility point $\eta_{\rm Carnot} = 1 - T_c/T_h$ is *formally* equated to the *hypothetical* efficiency bound of WOF had it been reversible, i.e., free of measurement costs, $\eta_{\rm reverse} \equiv 1 - E_{\rm rem}/E_{\rm in}$. Yet, even with this choice, HE and WOF can perform very differently: HE power production vanishes at the Carnot bound, and the efficiency bound at the maximal work point of generic HE can be much lower [52–57] (SM, VIII [23]), whereas $\eta_{\rm reverse}$ is similar to the bound $\eta_{\rm max}^{(1)}$ of the WOF that corresponds to maximal work production $\eta_{\rm reverse} \simeq \eta_{\rm max}^{(1)} \simeq \eta \simeq 1 - O(1/\sqrt{\bar{n}})$ for $\bar{n} \gg 1$ [Fig. 2(c)]. In general, there is an inherent (model-dependent) trade-off between HE power and efficiency [52–60], since the work and power production are reduced at excessively short cycles due to friction or incomplete heat exchange with the heat baths [52,53]. By contrast, there is no such trade-off in WOF, where power grows with the process rate provided it is less than $1/\tau_{\rm reset}$. Therefore, WOF may in principle outperform common HE with same resources, e.g., the Otto HE (SM, VIII [23]). A fully quantitative comparison of HE and WOF is unfeasible since the efficiency and power output of realistic HEs are generally lower than the theoretical bounds [52,53,60], partly due to the on- and off-switching of their coupling to heat baths and to controlling the adiabatic steps [61–63] whose energy cost must be accounted for. Likewise, the WOF feedforward cost cannot be simply estimated (see below).

For a given $E_{\rm in} = k_B T \gg \hbar\omega (\bar{n} \gg 1)$, the upper bounds on work production efficiency in our WOF scheme may well surpass those of a Szilard or Maxwell-demon binary decision engine energized by thermal-noise photodetection [40], since WOF consumes only a $O(1/\sqrt{\bar{n}})$ fraction of the input, whereas its Szilard counterpart consumes a fraction comparable to 1 (SM, VII [23]). For $T \to \infty$ (the classical limit), WOF is at its best, since homodyning then does not require photon counting but merely snapshots with negligible energy cost. For example, if a thermal ensemble of classical pendula with mean energy of 1 erg and frequency of 1 Hz contains $\bar{n} \sim 10^{27}$ (which need not be counted, only the pendula motion needs to be photographed for WOF), WOF then has ~ 1–10^{-13} efficiency, which can hardly be surpassed by other methods! With currently available detector efficiency $\kappa_D^2 \gtrsim 0.9$ and temperature $T_D \lesssim 1$ mK [45,46], only a few photons, $\bar{n} \lesssim 10$, suffice to generate work output, i.e., a much less noisy signal than the input [Fig. 2(c)]. The hard lower bound on $W_{\rm net}$ production is the Landauer resetting bound (SM, VI [23]). Since the reset energy cost is currently ca. tenfold [45,46], $\bar{n} \gtrsim 10^2$ practically ensure $\eta > 0$ in Eq. (5).

By definition, *all information engines*, including WOF, have technical energy costs of signal processing and the conversion of this information into physical manipulations required for feedforward, but these costs are commonly disregarded [32–44,64–66]. One can treat such technical costs as extra energy consumption that sets the threshold for “autonomous” WOF. Yet, these thresholds are strongly setup-dependent and therefore cannot be generally quantified. Thus, standard photodetection and electro-optical feedforward techniques can be replaced by all-optical techniques that may demand much less energy: (1) *quantum-nondemolition photon counting* of the signal by an optical probe in Rydberg polaritonic media [67–71]; (2) output signal processing by unconventional *heat-powered* transistors [72–74]; and (3) photorefractive beam splitters that can control the output quadrature shifts by signal-pump interference [75].

The WOF scheme is generally applicable to any noisy source (not only thermal) where homodyning of continuous variables can be performed, e.g., in ultracold bosonic gases where homodyning was proposed [76] and demonstrated [77]. Homodyning is also feasible via photocurrents induced by signal-pump interference in semiconductors [78,79] and for phonon fields in acoustic structures [80–84]. Any such setup allows one to split off a small fraction of the input field and mix it with a correspondingly weak coherent LO, thereby yielding work as per Eqs. (3)–(5). Thus, the proposed WOF may open new paths toward the exploitation of continuous-variable noise as a source of useful work in both classical and quantum regimes of diverse systems.

We thank O. Firstenberg and E. Poem of WIS for useful comments on the manuscript. We acknowledge the support of NSF-BSF, DFG, QUANTERA section of ERANET (PACE-IN), FET-Open (PATHOS), and ISF. T. O. is supported by the Czech Science Foundation, Grant No. 20-27994S.

*Corresponding author.
avijitmisra0120@gmail.com

[1] C. W. Gardiner and P. Zoller, *Quantum Noise* (Springer, Berlin, 2000).
[2] R. Alicki, The quantum open system as a model of the heat engine, J. Phys. A **12**, L103 (1979).
[3] P. Talkner, E. Lutz, and P. Hänggi, Fluctuation theorems: Work is not an observable, Phys. Rev. E **75**, 050102(R) (2007).
[4] W. Pusz and S. L. Woronowicz, Passive states and kms states for general quantum systems, Commun. Math. Phys. **58**, 273 (1978).
[5] D. Gelbwaser-Klimovsky, R. Alicki, and G. Kurizki, Work and energy gain of heat-pumped quantized amplifiers, Europhys. Lett. **103**, 60005 (2013).
[6] D. Gelbwaser-Klimovsky and G. Kurizki, Heat-machine control by quantum-state preparation: From quantum engines to refrigerators, Phys. Rev. E **90**, 022102 (2014).
[7] D. Gelbwaser-Klimovsky, W. Niedenzu, and G. Kurizki, Thermodynamics of quantum systems under dynamical control, Adv. At. Mol. Opt. Phys. **64**, 329 (2015).
[8] W. Niedenzu, V. Mukherjee, A. Ghosh, A. G. Kofman, and G. Kurizki, Quantum engine efficiency bound beyond the second law of thermodynamics, Nat. Commun. **9**, 165 (2018).
[9] M. E. Ronald Waynant, *Quantum Optics* (McGraw Hill Professional, Cambridge, UK, 1997).
[10] M. G. A. Paris, Quantum estimation for quantum technology, arXiv:0804.2981.
[11] W. Schleich, *Quantum Optics in Phase Space* (Wiley-VCH, New York, 2001).
[12] M. O. Scully and M. S. Zubairy, *Quantum Optics* (Cambridge University Press, Cambridge, England, 1997).
[13] H. Carmichael, *Statistical Methods in Quantum Optics* (Springer, Berlin, 1999).
[14] D. F. Walls and G. J. Milburn, *Quantum Optics*, 1st ed. (Springer-Verlag, Berlin, 1994).
[15] U. Leonhardt, *Measuring the Quantum State of Light* (Cambridge Studies in Modern Optics, Cambridge, 1997).
[16] M. G. A. Paris, Homodyne photocurrent, symmetries in photon mixing and number state synthesis, Int. J. Mod. Phys. B **11**, 1913 (1997).
[17] A. E. Allahverdyan and Th. M. Nieuwenhuizen, Extraction of Work from a Single Thermal Bath in the Quantum Regime, Phys. Rev. Lett. **85**, 1799 (2000).
[18] E. G. Brown, N. Friis, and M. Huber, Passivity and practical work extraction using gaussian operations, New J. Phys. **18**, 113028 (2016).
[19] R. Uzdin and S. Rahav, Global Passivity in Microscopic Thermodynamics, Phys. Rev. X **8**, 021064 (2018).
[20] D. Gelbwaser-Klimovsky and G. Kurizki, Work extraction from heat-powered quantized optomechanical setups, Sci. Rep. **5**, 7809 (2015)).
[21] A. Ghosh, C. L. Latune, L. Davidovich, and G. Kurizki, Catalysis of heat-to-work conversion in quantum machines, Proc. Natl. Acad. Sci. U.S.A. **114**, 12156 (2017).
[22] A. Ghosh, D. Gelbwaser-Klimovsky, W. Niedenzu, A. I. Lvovsky, I. Mazets, M. O. Scully, and G. Kurizki, Two-level masers as heat-to-work converters, Proc. Natl. Acad. Sci. U.S.A. **115**, 9941 (2018).
[23] See Supplemental Material, which contains Refs. [24,25], at http://link.aps.org/supplemental/10.1103/PhysRevLett.127.040602 for a detailed derivation, including spurious noise, and a comparison with information and heat engines.
[24] J. G. Skellam, The frequency distribution of the difference between two poisson variates belonging to different populations, J. R. Stat. Soc. **109**, 296 (1946).
[25] W. Shockley and H. J. Queisser, Detailed balance limit of efficiency of p-n junction solar cells, J. Appl. Phys. **32**, 510 (1961).
[26] R. Landauer, Irreversibility and heat generation in the computing process, IBM J. Res. Dev. **5**, 183 (1961).
[27] A. Berut, A. Arakelyan, A. Petrosyan, S. Ciliberto, R. Dillenschneider, and E. Lutz, Experimental verification of

Landauer's principle linking information and thermodynamics, Nature (London) **483**, 187 (2012).
[28] E. Lutz and S. Ciliberto, Information: From Maxwells demon to Landauers eraser, Phys. Today **68**, No. 9, 30 (2015).
[29] J. Goold, M. Paternostro, and K. Modi, Nonequilibrium Quantum Landauer Principle, Phys. Rev. Lett. **114**, 060602 (2015).
[30] P. Faist, F. Dupuis, J. Oppenheim, and R. Renner, The minimal work cost of information processing, Nat. Commun. **6**, 7669 (2015).
[31] R. Alicki, Quantum memories and Landauer's principle, arXiv:1007.1089.
[32] J. C. Maxwell, *Theory of Heat* (Longman, London, UK, 1871).
[33] L. Szilard, über die entropieverminderung in einem thermodynamischen system bei eingriffen intelligenter wesen, Z. Phys. **53**, 840 (1929).
[34] T. Sagawa and M. Ueda, Second Law of Thermodynamics with Discrete Quantum Feedback Control, Phys. Rev. Lett. **100**, 080403 (2008).
[35] S. W. Kim, T. Sagawa, S. De Liberato, and M. Ueda, Quantum Szilard Engine, Phys. Rev. Lett. **106**, 070401 (2011).
[36] J. J. Park, K.-H. Kim, T. Sagawa, and S. W. Kim, Heat Engine Driven by Purely Quantum Information, Phys. Rev. Lett. **111**, 230402 (2013).
[37] J. M. Diaz de la Cruz and M. A. Martin-Delgado, Quantum-information engines with many-body states attaining optimal extractable work with quantum control, Phys. Rev. A **89**, 032327 (2014).
[38] J. M. R. Parrondo, J. M. Horowitz, and T. Sagawa, Thermodynamics of information, Nat. Phys. **11**, 131 (2015).
[39] J. Goold, M. Huber, A. Riera, L. del Rio, and P. Skrzypczyk, The role of quantum information in thermodynamics—a topical review, J. Phys. A **49**, 143001 (2016).
[40] M. D. Vidrighin, O. Dahlsten, M. Barbieri, M. S. Kim, V. Vedral, and I. A. Walmsley, Photonic Maxwell's Demon, Phys. Rev. Lett. **116**, 050401 (2016).
[41] K. Beyer, K. Luoma, and W. T. Strunz, Steering Heat Engines: A Truly Quantum Maxwell Demon, Phys. Rev. Lett. **123**, 250606 (2019).
[42] J. Bengtsson, M. N. Tengstrand, A. Wacker, P. Samuelsson, M. Ueda, H. Linke, and S. M. Reimann, Quantum Szilard Engine with Attractively Interacting Bosons, Phys. Rev. Lett. **120**, 100601 (2018).
[43] K. Chida, S. Desai, K. Nishiguchi, and A. Fujiwara, Power generator driven by maxwell's demon, Nat. Commun. **8**, 15310 (2017).
[44] A. Aydin, A. Sisman, and R. Kosloff, Landauers principle in a quantum Szilard engine without Maxwells demon, Entropy **22**, 294 (2020).
[45] C. M. Natarajan, M. G. Tanner, and R. H. Hadfield, Superconducting nanowire single-photon detectors: physics and applications, Supercond. Sci. Technol. **25**, 063001 (2012).
[46] M. A. Wolff, S. Vogel, L. Splitthoff, and C. Schuck, Superconducting nanowire single-photon detectors integrated with tantalum pentoxide waveguides, Sci. Rep. **10**, 17170 (2020).
[47] R. Gaudenzi, E. Burzurí, S. Maegawa, H. S. J. van der Zant, and F. Luis, Quantum Landauer erasure with a molecular nanomagnet, Nat. Phys. **14**, 565 (2018).
[48] N. Erez, G. Gordon, M. Nest, and G. Kurizki, Thermodynamic control by frequent quantum measurements, Nature (London) **452**, 724 (2008).
[49] G. Gordon, G. Bensky, D. Gelbwaser-Klimovsky, D D Bhaktavatsala Rao, N. Erez, and G. Kurizki, Cooling down quantum bits on ultrashort time scales, New J. Phys. **11**, 123025 (2009).
[50] G. A. Álvarez, D. D. B. Rao, L. Frydman, and G. Kurizki, Zeno and Anti-Zeno Polarization Control of Spin Ensembles by Induced Dephasing, Phys. Rev. Lett. **105**, 160401 (2010).
[51] V. Mukherjee, A. G. Kofman, and G. Kurizki, Anti-Zeno quantum advantage in fast-driven heat machines, Commun. Phys. **3**, 8 (2020).
[52] R. Kosloff and Y. Rezek, The quantum harmonic otto cycle, Entropy **19**, 136 (2017).
[53] Y. Rezek and R. Kosloff, Irreversible performance of a quantum harmonic heat engine, New J. Phys. **8**, 83 (2006).
[54] D. G-Klimovsky, W. Niedenzu, and G. Kurizki, Thermodynamics of quantum systems under dynamical control, Adv. At. Mol. Opt. Phys. **64**, 329 (2015).
[55] R. Kosloff, Quantum thermodynamics: A dynamical viewpoint, Entropy **15**, 2100 (2013).
[56] B. Lin and J. Chen, Performance analysis of an irreversible quantum heat engine working with harmonic oscillators, Phys. Rev. E **67**, 046105 (2003).
[57] S. H. Raja, S. Maniscalco, G.-S. Paraoanu, J. P. Pekola, and N. L. Gullo, Finite-time quantum Stirling heat engine, arXiv:2009.10038.
[58] I. I. Novikov, The efficiency of atomic power stations (a review), J. Nucl. Energy (1954) **7**, 125 (1958).
[59] F. L. Curzon and B. Ahlborn, Efficiency of a carnot engine at maximum power output, Am. J. Phys. **43**, 22 (1975).
[60] T. Feldmann, E. Geva, R. Kosloff, and P. Salamon, Heat engines in finite time governed by master equations, Am. J. Phys. **64**, 485 (1996).
[61] M. Beau, J. Jaramillo, and A. Del Campo, Scaling-up quantum heat engines efficiently via shortcuts to adiabaticity, Entropy **18**, 168 (2016).
[62] B. Çakmak and Ö. E. Müstecaplıoğlu, Spin quantum heat engines with shortcuts to adiabaticity, Phys. Rev. E **99**, 032108 (2019).
[63] R. Kosloff and Y. Rezek, The quantum harmonic otto cycle, Entropy **19**, 136 (2017).
[64] C. Elouard and A. N. Jordan, Efficient Quantum Measurement Engines, Phys. Rev. Lett. **120**, 260601 (2018).
[65] C. Elouard, D. Herrera-Martí, B. Huard, and A. Auffèves, Extracting Work from Quantum Measurement in Maxwell's Demon Engines, Phys. Rev. Lett. **118**, 260603 (2017).
[66] S. Seah, S. Nimmrichter, and V. Scarani, Maxwell's Lesser Demon: A Quantum Engine Driven by Pointer Measurements, Phys. Rev. Lett. **124**, 100603 (2020).
[67] I. Friedler, D. Petrosyan, M. Fleischhauer, and G. Kurizki, Long-range interactions and entanglement of slow single-photon pulses, Phys. Rev. A **72**, 043803 (2005).

[68] E. Shahmoon, G. Kurizki, M. Fleischhauer, and D. Petrosyan, Strongly interacting photons in hollow-core waveguides, Phys. Rev. A **83**, 033806 (2011).

[69] A. V. Gorshkov, J. Otterbach, M. Fleischhauer, T. Pohl, and M. D. Lukin, Photon-Photon Interactions via Rydberg Blockade, Phys. Rev. Lett. **107**, 133602 (2011).

[70] O. Firstenberg, T. Peyronel, Q.-Y. Liang, A. V. Gorshkov, M. D. Lukin, and V. Vuletić, Attractive photons in a quantum nonlinear medium, Nature (London) **502**, 71 (2013).

[71] D. Tiarks, S. Schmidt-Eberle, T. Stolz, G. Rempe, and S. Dürr, A photon–photon quantum gate based on Rydberg interactions, Nat. Phys. **15**, 124 (2019).

[72] K. Joulain, J. Drevillon, Y. Ezzahri, and J. Ordonez-Miranda, Quantum Thermal Transistor, Phys. Rev. Lett. **116**, 200601 (2016).

[73] C. Wang, D. Xu, H. Liu, and X. Gao, Thermal rectification and heat amplification in a nonequilibrium v-type three-level system, Phys. Rev. E **99**, 042102 (2019).

[74] M. T. Naseem, A. Misra, Ö. E. Müstecaplioğlu, and G. Kurizki, Minimal quantum heat manager boosted by bath spectral filtering, Phys. Rev. Research **2**, 033285 (2020).

[75] R. W. Boyd, *Nonlinear Optics* (Academic Press, Burlington, 2008).

[76] N. Bar-Gill, C. Gross, I. Mazets, M. Oberthaler, and G. Kurizki, Einstein-Podolsky-Rosen Correlations of Ultracold Atomic Gases, Phys. Rev. Lett. **106**, 120404 (2011).

[77] C. Gross, H. Strobel, E. Nicklas, T. Zibold, N. Bar-Gill, G. Kurizki, and M. K. Oberthaler, Atomic homodyne detection of continuous-variable entangled twin-atom states, Nature (London) **480**, 219 (2011).

[78] G. Kurizki, M. Shapiro, and P. Brumer, Phase-coherent control of photocurrent directionality in semiconductors, Phys. Rev. B **39**, 3435 (1989).

[79] G. Kurizki and M. Shapiro, Detection of squeezed light by directional photoionization of coherently superposed states with different symmetries, J. Opt. Soc. Am. B **8**, 355 (1991).

[80] *Phononic Crystals: Fundamentals and Applications*, 1st ed., edited by A. Khelif and A. Adibi (Springer, New York, 2015).

[81] *Acoustic Metamaterials and Phononic Crystals*, 2013th ed., edited by P. A. Deymier (Springer, Berlin; New York, 2013).

[82] M. S. Kushwaha, P. Halevi, L. Dobrzynski, and B. Djafari-Rouhani, Acoustic Band Structure of Periodic Elastic Composites, Phys. Rev. Lett. **71**, 2022 (1993).

[83] A. Khelif, B. Djafari-Rouhani, J. O. Vasseur, and P. A. Deymier, Transmission and dispersion relations of perfect and defect-containing waveguide structures in phononic band gap materials, Phys. Rev. B **68**, 024302 (2003).

[84] T. Elnady, A. Elsabbagh, W. Akl, O. Mohamady, V. M. Garcia-Chocano, D. Torrent, F. Cervera, and J. Sánchez-Dehesa, Quenching of acoustic bandgaps by flow noise, Appl. Phys. Lett. **94**, 134104 (2009).